


METHODOLOGY

Open Access



PACER: a novel 3D plant cell wall model for the analysis of non-catalytic and enzymatic responses

Mareike Monschein¹, Edita Jurak^{1,2}, Tanja Paasela³, Taru Koitto¹, Vera Lambauer¹, Mirko Pavicic³, Thomas Enjalbert⁴, Claire Dumon⁴ and Emma R. Master^{1,5*} 

Abstract

Background: Substrate accessibility remains a key limitation to the efficient enzymatic deconstruction of lignocellulosic biomass. Limited substrate accessibility is often addressed by increasing enzyme loading, which increases process and product costs. Alternatively, considerable efforts are underway world-wide to identify amorphogenesis-inducing proteins and protein domains that increase the accessibility of carbohydrate-active enzymes to targeted lignocellulose components.

Results: We established a three-dimensional assay, PACER (plant cell wall model for the analysis of non-catalytic and enzymatic responses), that enables analysis of enzyme migration through defined lignocellulose composites. A cellulose/azo-xylan composite was made to demonstrate the PACER concept and then used to test the migration and activity of multiple xylanolytic enzymes. In addition to non-catalytic domains of xylanases, the potential of loosenin-like proteins to boost xylanase migration through cellulose/azo-xylan composites was observed.

Conclusions: The PACER assay is inexpensive and parallelizable, suitable for screening proteins for ability to increase enzyme accessibility to lignocellulose substrates. Using the PACER assay, we visualized the impact of xylan-binding modules and loosenin-like proteins on xylanase mobility and access to targeted substrates. Given the flexibility to use different composite materials, the PACER assay presents a versatile platform to study impacts of lignocellulose components on enzyme access to targeted substrates.

Keywords: Xylanase, Loosenin, Assay development, Enzyme accessibility, Amorphogenesis, Xylan, Lignocellulose

Background

The past 20 years has marked several major breakthroughs in our fundamental understanding of lignocellulose bioconversion [1–3]. Some of these breakthroughs are already incorporated in enzyme formulations for the efficient conversion of lignocellulosic biomass to fuels, chemicals and new bio-based materials [4–6]. Despite the tremendous achievements by excellent research

groups world-wide, currently available enzyme formulations fall short of transformation efficiencies achieved in nature. As a result, the economic feasibility of lignocellulose bioconversion to fuels and chemicals remains a challenge [7–9]. In particular, limited accessibility of isolated enzymes to targeted lignocellulose components is acknowledged as a major hurdle to enzymatic deconstruction of biomass [10–14].

Enzyme accessibility to targeted substrates embedded in lignocellulosic fiber (e.g., cellulase accessibility to cellulose) has been correlated to the interior surface area of the fiber (i.e., pore size and pore size distribution) as well as exterior surface area of the fiber (i.e.,

*Correspondence: emma.master@aalto.fi

¹ Department of Bioproducts and Biosystems, Aalto University, Kemistintie 1, 02150 Espoo, Finland

Full list of author information is available at the end of the article



© The Author(s) 2022. **Open Access** This article is licensed under a Creative Commons Attribution 4.0 International License, which permits use, sharing, adaptation, distribution and reproduction in any medium or format, as long as you give appropriate credit to the original author(s) and the source, provide a link to the Creative Commons licence, and indicate if changes were made. The images or other third party material in this article are included in the article's Creative Commons licence, unless indicated otherwise in a credit line to the material. If material is not included in the article's Creative Commons licence and your intended use is not permitted by statutory regulation or exceeds the permitted use, you will need to obtain permission directly from the copyright holder. To view a copy of this licence, visit <http://creativecommons.org/licenses/by/4.0/>. The Creative Commons Public Domain Dedication waiver (<http://creativecommons.org/publicdomain/zero/1.0/>) applies to the data made available in this article, unless otherwise stated in a credit line to the data.

particle size) [14–18]. In addition to structural factors, the chemical composition and distribution of hemicelluloses and lignin in lignocellulosic substrates impacts enzyme accessibility [19–22]. Measurements of pore size distribution and exterior surface area of lignocellulose substrates include solute exclusion [23, 24], Simons' staining [10, 25], water retention [26], fiber size analysis [26] and thermoporosimetry [27]. Such methods have been especially beneficial when evaluating the impact of lignocellulose pretreatment and cellulose fiber processing on the performance of cellulolytic enzymes. Besides physicochemical analysis of different lignocellulose preparations, fluorescence microscopy, atomic force microscopy, scanning electron microscopy (SEM) among other imaging techniques are powerful options for monitoring changes to fiber structure and accessibility during enzymatic processing [12, 28–31]. Such imaging approaches, however, are impractical for screening new amorphogenesis-inducing proteins that boost the enzymatic deconstruction of lignocellulose.

The term amorphogenesis was introduced in 1985 to describe the first step to cellulose deconstruction by hydrolytic enzymes [32]. Non-hydrolytic proteins and protein domains that potentially play a role in amorphogenesis increase the initial accessibility of carbohydrate-active enzymes to lignocellulosic substrates [15]. Reported examples include certain carbohydrate-binding modules (CBMs) [33], swollenins [34–36], loosenins [37, 38], microbial expansin-like proteins [38–41] and lytic polysaccharide monoxygenases [42]. Since amorphogenesis-inducing proteins often adopt a non-hydrolytic mode of action, we contend functional screens that rely solely on the detection of soluble products risk overlooking those proteins that impact enzyme accessibility and migration through lignocellulose materials. Accordingly, our aim was to establish a versatile and low-cost approach to screen for proteins that impact the accessibility of glycoside hydrolases to targeted lignocellulose components.

Herein, we introduce the PACER assay, a novel 3D Plant cell wall model for the Analysis of non-Catalytic and Enzymatic Responses. The PACER assay was inspired by a three-dimensional human cell culture system [43] and establishes a versatile new screen for proteins that impact the migration of glycoside hydrolases and other enzymes through model lignocellulosic materials. This technique allows the visualization of enzyme penetration and migration along a constructed cellulose composite, and impacts of non-catalytic proteins and protein modules on enzyme migration. Three lines of investigation were pursued for proof of concept of the PACER assay: (1) comparative analysis of three *endo*-1,4- β -xylanases to assess the impact of protein size and presence of a CBM

on enzyme migration through a formulated cellulose/azo-xylan matrix; (2) evaluation of two loosenins for their potential to increase xylanase migration through the formulated matrix, and (3) characterization of *Pm25*, an *endo*-1,4- β -xylanase recently discovered from termite gut metagenome [44]. By simultaneously measuring product release and migration of enzymes through defined cellulosic materials, the PACER assay can uncover determinants of enzyme accessibility not detected through measuring release of soluble products alone.

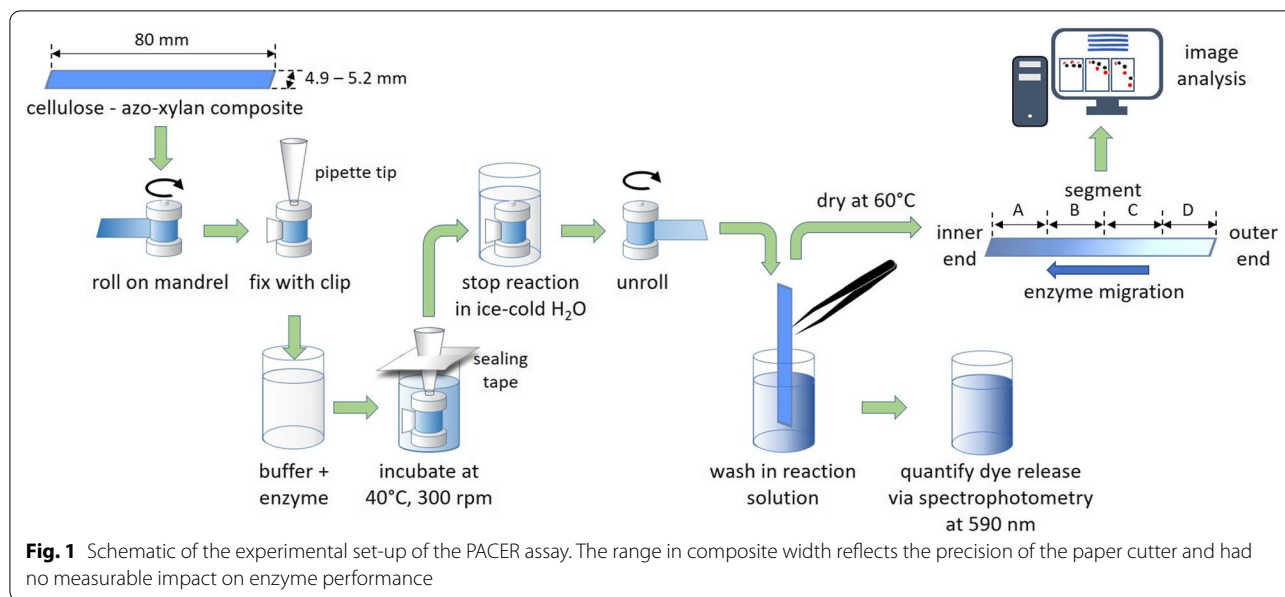
Results and discussion

Development of the PACER assay

Heteroxylans are a diverse group of branched xylans with a backbone of β -(1 \rightarrow 4)-linked D-xylopyranosyl (Xylp) residues that can be substituted with α -L-arabinofuranose (Araf), 4-O-methyl- α -D-glucuronic acid (MeGlcAp), acetyl groups, *p*-coumaric acid and ferulic acid, depending on the botanical source [45]. After cellulose, xylans are the most abundant polysaccharide found in lignocellulosic biomass; accordingly, for proof of concept of the PACER assay, we used azo-coupled xylan from birchwood for the impregnation of filter paper (Fig. 1). To initially evaluate azo-xylan retention on the cellulose filter paper, azo-xylan solutions were prepared at between 2.5 and 10% w/v in either milli-Q water or 0.5 M NaOH, and the absorbance of remaining azo-xylan in solution was measured spectrophotometrically at 590 nm. Best retention was observed after solubilizing azo-xylan in 0.5 M NaOH and retention did not increase at azo-xylan concentrations above 5% w/v. Accordingly, the cellulose/azo-xylan composites were prepared using a 5% azo-xylan (w/v) solution prepared in 0.5 M NaOH; acid hydrolysis of corresponding composites confirmed $7.2 \pm 0.5\%$ w/w xylan in the generated materials.

Comparison of the accessibility and activity of three different xylanases

The PACER assay was used to compare three *endo*- β -1,4-xylanases differentiated by glycoside hydrolase family and occurrence of a family 2 carbohydrate-binding module type B (CBM2b). The enzymes were the glycoside hydrolase family 10 (GH10) xylanase from *Cellvibrio mixtus* (*CmXyn10B*; Megazyme), the GH11 xylanase from *Neocallimastix patriciarum* (*NpXyn11A*; Megazyme), and the GH11 xylanase from *Thermobifida fusca* (*TfXyn11A*) [46] that comprises a C-terminal carbohydrate-binding module belonging to CBM family 2 (CBM2b) (<http://www.cazy.org>) (Table 1). Briefly, GH10 *endo*-xylanases bind two consecutive unsubstituted Xylp residues and can generate terminally substituted xylo-oligosaccharides, whereas GH11 xylanases

**Table 1** Properties of enzymes used in this study

Enzyme	Organism	CAZY number	Molecular mass (kDa)	CBM	UNIPROT Accession number	Specific activity (U/mg)*
<i>CmXyn10B</i>	<i>Cellvibrio mixtus</i>	GH10	41.7	–	O68541	7.32
<i>NpXyn11A</i>	<i>Neocallimastix patriciarum</i>	GH11	25.8	–	P29127	14.2
<i>TfXyn11A</i>	<i>Thermobifida fusca</i>	GH11	31.9	CBM2b	Q47QL8	8.06
<i>Pm25</i> (WT)	Unclassified; from termite gut	GH10	83.9	CBM4	S0DFK9	0.29
<i>Pm25</i> Y213A Y378A (M5)	metagenome		83.8	CBM4		0.29
<i>Pm25</i> ΔCBMs (M6)			48.8	–		0.49
<i>Pm25</i> E546A (M1)			83.9	CBM4		0.01

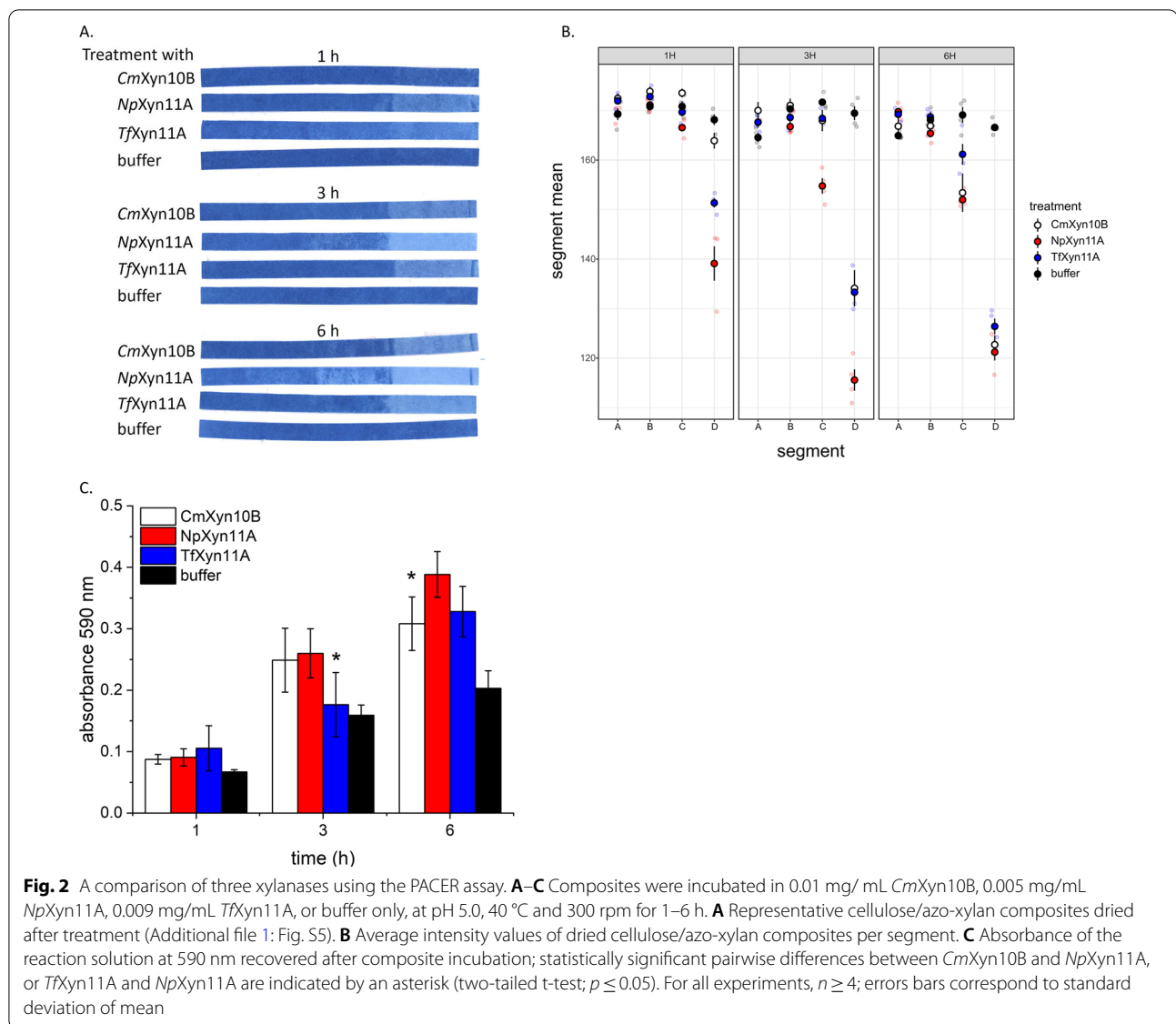
* Determined using azo-xylan at pH 5.0 and 40 °C

require three consecutive unsubstituted Xylp residues and can generate internally substituted xylo-oligosaccharides [47, 48].

Following treatment with all three *endo*-β-1,4-xylanases, the cellulose/azo-xylan composite used in the PACER assay showed a discolouration that progressed over time from the right edge to the left edge of the strip (Fig. 2A, B). This was caused by enzymatic release of azo-coupled oligosaccharides and corresponds to enzyme migration from the outer layer (segment D) towards the inner layers (segment C-A) of the composite when rolled around the mandrel. Overall, *NpXyn11A* migrated fastest and furthest through the cellulose/azo-xylan composite. The greater migration of *NpXyn11A* compared to *CmXyn10B* and *TfXyn11A* was detected after each time point (Fig. 2A, B), even though *CmXyn10B* and *TfXyn11A* released similar levels of soluble product to *NpXyn11A*

after 1 h, and even after 3 h in the case of *CmXyn10B* (Fig. 2C).

This comparative analysis underscores the problem with equating soluble product release and enzyme accessibility to the corresponding substrate. Given that enzyme loadings used herein were based on units of activity, we reasoned that the different positions targeted by GH10 and GH11 would have negligible impact on enzyme migration through the constructed composites. Instead, the presence of a CBM, size of the catalytic domain, and number of Xylp binding sites, likely impacted the diffusion of *TfXyn11A*, *NpXyn11A* and *CmXyn10B*. *TfXyn11A* (32 kDa) contains a C-terminal CBM2b that binds both cellulose and insoluble xylan [46]. As a type B CBM, CBM2b of *TfXyn11A* is expected to primarily target the enzyme to the substrate (i.e., display a so-called targeting function) rather than promote fiber disruption [49, 50]. Accordingly, *TfXyn11A* migration through the cellulose/



azo-xylan composite could be limited by dissociation from the substrate. Since neither *CmXyn10B* (42 kDa) or *NpXyn11A* (26 kDa) comprise a CBM, the difference in their molecular weight likely drove the varying migration of these enzymes. It is also conceivable that the extended substrate binding surface formed by the higher number of *Xylp* binding sub-sites expected in *NpXyn11A* compared to *CmXyn10B* increased *NpXyn11A* accessibility to the xylan substrate within the cellulose/azo-xylan composite. Future mutagenesis studies of *NpXyn11A*, for example, could apply the PACER assay to directly evaluate the impact of an extended substrate binding site on substrate accessibility.

Impact of loosenin-like proteins on *NpXyn11A* migration
NpXyn11A demonstrated greatest migration through the cellulose/azo-xylan composites and so was selected to investigate the potential of two loosenin-like proteins (*PcaLOOL2* and *PcaLOOL12* from *Phanerochaete carnosae*) for ability to boost enzyme accessibility to the xylan substrate [51]. Briefly, loosenins and loosenin-like proteins are microbial expansin-related proteins that comprise the N-terminal D1 domain characteristic of microbial and plant expansins [37, 52]. Similar to other microbial expansin-related proteins, loosenins reportedly weaken filter paper, disrupt cotton fibers, and boost cellulase action on lignocellulosic substrates by a non-lytic mechanism [37, 38].

Using the PACER assay, we observed the potential of PcaLOOL2 and PcaLOOL12 to increase *NpXyn11A* migration through the constructed cellulose/azo-xylan composite. After 3 h of incubation, *NpXyn11A* migration through the composites was more advanced in those pretreated with either PcaLOOL2 or PcaLOOL12 compared to composites pretreated with bovine serum albumin (BSA) (Fig. 3A, B). Moreover, the increased migration of *NpXyn11A* through composites pretreated with PcaLOOL2 coincided with an increase in absorbance measurements of the resulting reaction solutions (Fig. 3C). Notably, the particular boosting effect of PcaLOOL2 on *NpXyn11A* activity was not observed using azo-xylan in solution (Additional file 1: Fig. S1), and consistent with the predicted loosening effect of loosenin-like proteins, control reactions lacking *NpXyn11A* showed low release of azo-xylan from composites treated with PcaLOOL2 and PcaLOOL12 alone (Additional file 1: Fig. S2).

PACER for the characterization of a novel GH10 endo- β -1,4-xylanase and its mutants

Having demonstrated the potential of the PACER assay to uncover performance differences between well characterized xylanases, we then evaluated the potential of the assay to characterize a recently discovered multimodular xylanase. Briefly, the earlier metagenomic analysis of the fungus-growing termite, *Pseudacanthotermes militaris*, revealed a putative xylan utilization locus linked to the genus *Bacteroides* [53]. One of its open reading frames encodes a multimodular GH10, designated *P. militaris* 25 (*Pm25*). This enzyme is characterized by a discontinuous organization that includes the insertion of two tandem CBM4 domains (CBM4-1 and CBM4-2) within the catalytic GH10 xylanase domain (Table 1) [44].

To assess the impact of this unusual multidomain organization on enzyme migration, *Pm25* and three constructs with modular deletions or point mutations were characterized using the PACER assay. Variant M1 (*Pm25*

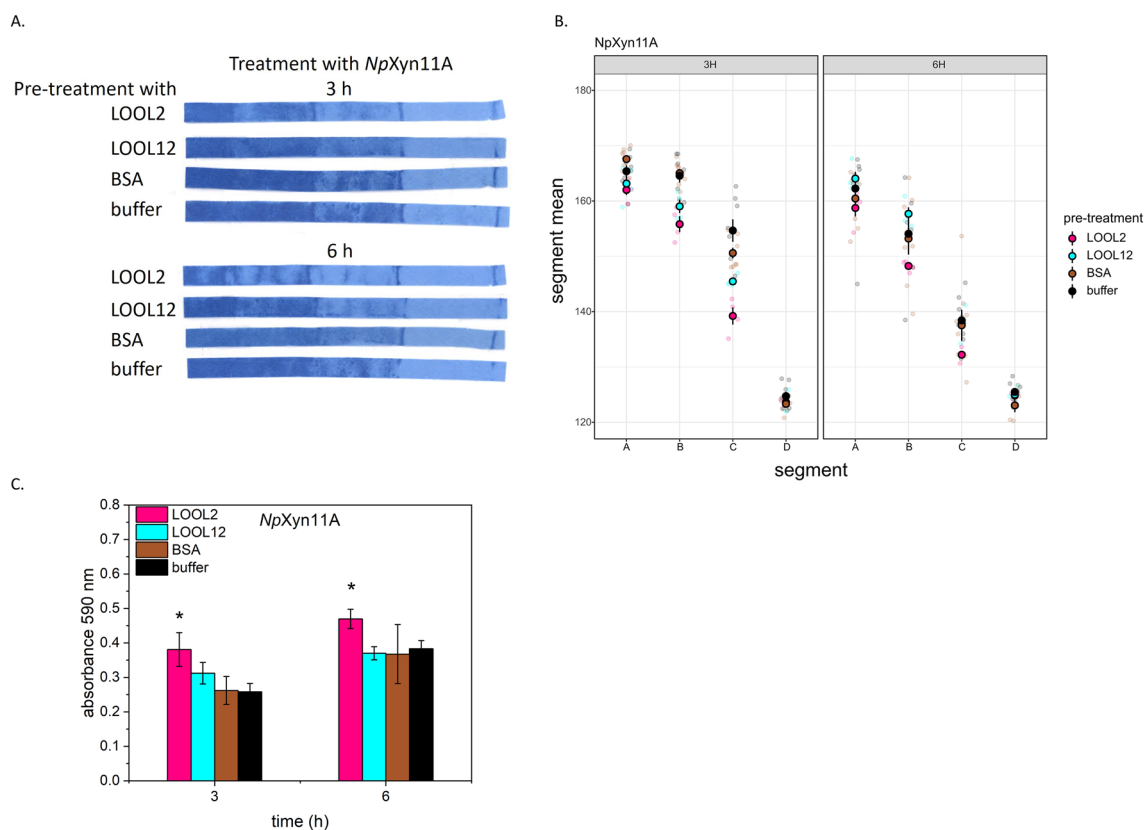


Fig. 3 Impact of loosenin-like proteins on *NpXyn11A* migration. Composites were pretreated with 0.1 mg/mL PcaLOOL2, PcaLOOL12, BSA or buffer only at pH 5.0 and room temperature for 24 h. This was followed by incubation in 0.005 mg/mL *NpXyn11A* or buffer only, at pH 5.0, 40 °C and 300 rpm for 3–6 h. **A** Representative cellulose/azo-xylan composites dried after treatment. **B** Average intensity values of dried cellulose/azo-xylan composites per segment. **C** Absorbance of the reaction solution at 590 nm recovered after composite incubation; statistically significant differences compared to pretreatment with BSA are indicated by an asterisk (two-tailed t-test; $p \leq 0.05$). For all experiments, $n \geq 4$; error bars correspond to standard deviation of mean

E546A) harbors a point mutation in domain GH10b, reducing its activity on glucuronoxylan and arabinoxylan by two to three orders of magnitude [44]. Variant M5 (*Pm25* Y213A + Y378A) carries two point mutations inactivating CBM4-1 and CBM4-2. Lastly, both CBM4 domains are deleted in M6 (*Pm25*ΔCBMs) [44]. Given the particularly low activity of M1 on azo-xylan in solution (Table 1), the wild-type *Pm25* and all variants were compared using the PACER assay on a molar basis.

The low residual activity of the M1 variant was insufficient to promote detectable M1 migration through the cellulose/azo-xylan composite (Fig. 4A, B). More interesting, despite achieving similar levels of azo-xylan hydrolysis in solution (Additional file 1: Fig. S3), differences in wild-type *Pm25*, M5 and M6 performance after 3 h were clearly observed when using the PACER assay

(Fig. 4A, B). The PACER assay also showed a clear correlation between activity and mobility, suggesting little to no passive diffusion of the enzyme through the system. The deletion of CBM4-1 and CBM4-2 leading to M6 significantly increased xylanase migration through the cellulose/azo-xylan composite, indicating that molecular weight outweighs the proximity effect gained by CBM4-1 and CBM4-2, at least at high substrate concentration [44]. Given the high apparent substrate concentration, the substantially lower migration of M5 compared to wild-type *Pm25* was more surprising. Wu et al. [44] previously reported the lower activity of M5 compared to wild-type *Pm25* on insoluble wheat bran; however, herein, differences in M5 and wild-type *Pm25* migration were observed despite displaying similar levels of activity on azo-xylan (Fig. 4C). It is conceivable

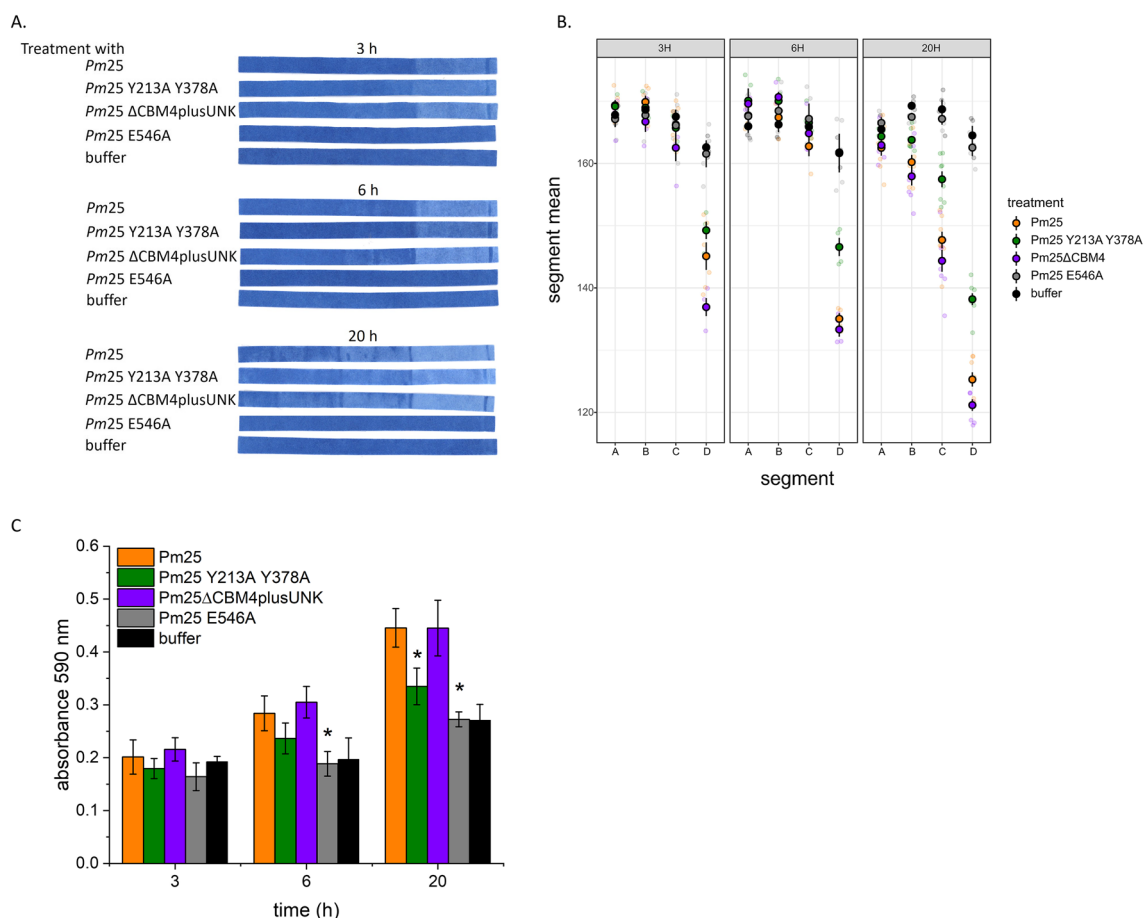


Fig. 4 Characterization of the novel GH10 xylanase *Pm25* and its mutants. Composites were incubated in 0.03 mg/ mL wild-type *Pm25*, 0.03 mg/ mL variant M5 (*Pm25* Y213A + Y378A), 0.017 mg/ mL variant M6 (*Pm25*ΔCBMs), 0.03 mg/ mL variant M1 (*Pm25* E546A), or buffer only, at pH 5.0, 40 °C and 300 rpm for 3–20 h. **A** Representative cellulose/azo-xylan composites dried after treatment. **B** Average intensity values of dried cellulose/azo-xylan composites per segment. **C** Absorbance of the reaction solution at 590 nm recovered after composite incubation; statistically significant differences compared to the wild-type *Pm25* are indicated by an asterisk (two-tailed t-test; $p \leq 0.05$). For all experiments, $n \geq 4$; error bars correspond to standard deviation of mean

that active forms of CBM4-1 and/or CBM4-2 of *Pm25* could impart both proximity and disruption effects to the wild-type *Pm25* by extending the number of Xylp binding sub-sites of the catalytic domain.

Conclusions

The three-dimensional PACER assay was established to accelerate the discovery of non-catalytic proteins and protein domains that increase enzyme access to lignocellulosic substrates. Using a cellulose/azo-xylan composite to demonstrate the PACER concept, we could readily visualize the impact of xylan-binding modules and loosenin-like proteins on xylanase mobility and accessibility to the targeted substrate. The low cost, small scale, and option to create different composite materials, contribute to the advantages of the PACER assay. By using labeled proteins, composites could in future be constructed using defined and native lignocellulose components, and then visualized by tracking the labeled protein.

Methods

Substrates and chemicals

VWR[®] quantitative filter paper grade 454 (Cat.# 516-0857) was supplied by VWR (Radnor, PA, USA). Azo-xylan (birchwood powder; Cat.# S-AXBP) was obtained from Megazyme (Bray, Ireland). All other chemicals were reagent grade.

Enzymes and non-catalytic proteins

CmXyn10B (recombinant *endo*- β -1,4-xylanase from *Cellvibrio mixtus*; Cat.# E-XYNBCM) and *NpXyn11A* (recombinant *endo*- β -1,4-xylanase from *Neocallimastix patriciarum*; Cat.# E-XYLNP) were obtained from Megazyme. *TfXyn11A* (recombinant *endo*- β -1,4-xylanase from *Thermobifida fusca*) was kindly provided by T.V. Vuong [46]. All xylanases were purchased or recombinantly prepared as mono-component enzymes; protein purity was determined by SDS-PAGE (Additional file 1: Fig. S4). Bovine serum albumin (BSA) was obtained from Sigma-Aldrich (St. Louis, MO, USA; CAS# 9048-46-8).

PcaLOOL2 (loosenin-like protein 2 from *Phanerochaete carnosae*, GenBank code EKM55357.1) and PcaLOOL12 (loosenin-like protein 12 from *Phanerochaete carnosae*, GenBank code EKM51974.1) were recombinantly expressed in *Pichia pastoris* SMD1168H. Briefly, codon optimized genes encoding PcaLOOL2 or PcaLOOL12 were obtained as subcloned in pPICZ α A plasmids with a C-terminal 6 \times His tag (GenScript, Piscataway, NJ, USA). Transformants were grown in shake flasks in buffered glycerol-complex medium (BMGY; 100 mM potassium phosphate buffer (pH 6.0), 2% (w/v) peptone, 1% (w/v) yeast extract, 1.34% (w/v) yeast

nitrogen base, 4×10^{-5} % (w/v) biotin, 1% (v/v) glycerol) at 30 °C and 100 rpm until an OD₆₀₀ of ~6 and then induced in buffered methanol-complex medium (BMMY; BMGY containing 0.5% (v/v) methanol instead of glycerol). Secreted recombinant proteins were purified from culture supernatants by FPLC using a GE Healthcare His-Trap[™] FF Crude prepacked column (Thermo Fisher Scientific; Cat.# 11723219).

Pm25 (*Xyn10C*, *endo*- β -1,4-xylanase from the termite *Pseudacanthotermes militaris* gut metagenome, GenBank code CCO21036.1) and variants M6 (*Pm25* Δ CBMs), M5 (*Pm25* Y213A Y378A) and M1 (*Pm25* E546A) were recombinantly expressed in *E. coli* Rosetta[™] (DE3) pLysS as previously described [44].

Enzyme activity determination

The activity of *endo*- β -1,4-xylanases on azo-xylan was determined according to the protocol provided by Megazyme with minor alterations. In brief, a 1% solution of azo-xylan was prepared in milli-Q H₂O, 0.25 mL was transferred into a 15-mL Falcon[™] conical centrifuge tube and pre-equilibrated in a ThermoMixer C set at 40 °C. Enzymes were diluted in 100 mM sodium acetate buffer (pH 5.0), 0.25 mL buffered enzyme preparation were added to the azo-xylan solution and thoroughly mixed. Tubes were incubated at 40 °C for 10 min, after which reactions were terminated by addition of 1.75 mL 96% (v/v) ethanol with vigorous stirring. Tubes were incubated at room temperature for 10 min and again thoroughly mixed. In the case of reaction blanks, ethanol was added prior to enzyme addition. Supernatants were recovered by centrifugation (3000 rpm for 10 min) and absorbance was analyzed spectrophotometrically at 590 nm. Activities were calculated with the Megazyme Mega-Calc[™] using *Aspergillus niger endo*- β -xylanase as a reference.

Preparation of cellulose/azo-xylan composites and confirmation of xylan content

Azo-xylan was dissolved in slightly heated 0.5 M NaOH to produce a 5% (w/v) solution and then stirred at room temperature for 1 h before transferring 6 mL of the solution to the bottom of a glass petri dish (\varnothing 190 mm). A pre-dried filter paper (VWR[®] quantitative filter paper grade 454; \varnothing 185 mm) was then submerged in the solution and covered with an additional 5 mL of the azo-xylan preparation. An even pressure was then applied by gently pressing the submerged filter paper with a second petri dish that had a slightly smaller diameter. After applying pressure to both sides of the filter paper, the paper was left to incubate in the azo-xylan solution for two more minutes before being placed between paper towels to

remove excessive liquid. The resulting cellulose/azo-xylan composite was then dried for 10 min at 60 °C, washed in ~125 mL ice-cold 0.5 M acetic acid for 2 min, rinsed and washed in milli-Q H₂O for 10 min, and then dried over night at 60 °C. The cellulose/azo-xylan composite was then cut into 4.9–5.2 mm × 80 mm strips using a guillotine paper trimmer. The weight percent of azo-xylan retained in the filter paper was verified by acid hydrolysis of cellulose/azo-xylan composites ($n=2$). Briefly, for the acid hydrolysis, 10–11 mg of composite (two composites were analyzed in duplicate, $n=4$) was prehydrolyzed with 72% H₂SO₄ (0.45 mL) at 30 °C for 1 h and then hydrolyzed with 1 M H₂SO₄ (10.9 mL) at 100 °C for 3 h. Samples were diluted 50 times and analyzed by high performance anion exchange chromatography (HPAEC) on a Dionex Ultimate 6000 system (Thermo Scientific, Sunnyvale, CA, USA) equipped with a CarboPac PA-1 column (2 mm × 250 mm ID) in combination with a CarboPac PA-1 guard column (2 mm × 50 mm ID) and PAD detector. Elution of monosaccharides (0.25 mL min⁻¹) was performed with a multi-step-gradient using the following eluents: A: 0.1 M NaOH, B: 1 M NaOAc in 0.1 M NaOH, C: 0.2 M NaOH, and D: milli-Q water. Gradient was as follows: 0–20 min 16% A and 84% D; 20–25 min 45%A, 5%B, and 50%D; 15 min with 60%A and 40% B; 25–37 min 100% C (flow rate up to 0.35 mL min⁻¹ over the first 2 min), and 37–49 min 16%A, 84%D (flow rate decreased to 0.25 mL min⁻¹ over the first 2 min). The system was controlled using Chromeleon 7.2.9 software (Thermo Scientific, Sunnyvale, CA, USA).

PACER assay

Cellulose/azo-xylan composites were soaked in 50 mM sodium acetate buffer (pH 5.0) for 3 min and then each strip was rolled tightly around a metal mandrel (Ø 6.0 mm, height 15.1 mm) before securing the outer end of the strip with a custom-made plastic clip [43]. The resulting mandrels were then placed in a 24-well round bottom microplate and fixed in an upright position using a pipette tip (Agilent Technologies, Santa Clara, CA, USA; Cat.# 202061-300) (Fig. 1).

To compare the migration of three different *endo*-β-1,4-xylanases, mandrels were incubated in a total reaction volume of 3 mL containing 0.01 mg/ mL *CmXyn10B*, 0.005 mg/ mL *NpXyn11A* or 0.009 mg/ mL *TjXyn11A* in 50 mM sodium acetate buffer (pH 5.0). For all three enzymes, this corresponded to 71 mU/ mL. As a reference, mandrels were incubated in buffer only. Incubations were performed for 1–6 h on a ThermoMixer C set at 40 °C and 300 rpm.

The impact of loosenin-like proteins on the migration of *endo*-β-1,4-xylanases through cellulose/azo-xylan composites was investigated by submerging each strip

(4.9–5.2 mm × 80 mm) in 0.5 mL of 50 mM sodium acetate buffer (pH 5.0) alone or containing 0.1 mg/ mL PcaLOOL2, PcaLOOL12, or BSA. After 24 h, each composite strip was rolled on a mandrel and incubated in 3 mL of 50 mM sodium acetate buffer (pH 5.0) alone or containing 0.005 mg/ mL (71 mU/ mL) *NpXyn11A*. Incubations were performed for 0.5–6 h on a ThermoMixer C set at 40 °C and 300 rpm.

The PACER assay was also used to further characterize a novel GH10 *endo*-β-1,4-xylanase and its mutants. Here, mandrels were incubated in 3 mL of 50 mM sodium acetate buffer (pH 5.0) containing 0.03 mg/ mL wild-type *Pm25*, 0.03 mg/ mL of the M5 mutant (*Pm25* Y213A Y378A), 0.017 mg/ mL of the M6 mutant (*Pm25*ΔCBMs) or 0.03 mg/ mL of the M1 mutant (*Pm25* E546A). As a reference, mandrels were incubated in buffer only. Incubations were performed for 0.5–20 h on a ThermoMixer C set at 40 °C and 300 rpm.

After each incubation, the mandrel was transferred to ice-cold milli-Q H₂O for 3 min. Composites were then unrolled, washed three times in their corresponding reaction solution to release soluble products to the reaction supernatant, placed on a petri dish and dried over night at 60 °C. Absorbance of the reaction solution was analyzed spectrophotometrically at 590 nm.

Image analysis

Dried composites were scanned at 600 × 600 dpi using Canon image RUNNER Advance C5250i system. The image processing was done with Fiji software [54, 55]. The scanned RGB images were converted to Hue Saturation Brightness (HSB) color space. The strips were segmented from the background pixels in the saturation channel using “Threshold tool” by choosing pixels with minimum intensity value of 80 and maximum value of 255. The saturation channel was chosen for the analysis because it contained most of the tone loss due to the enzymatic reaction in comparison to the other channels. From Fiji function “Analyze particles” the minimum particle size was set as 1000 pixels to remove wrongly selected pixels from the background. Fiji function “save XY coordinates” was used to extract the x and y coordinates of each pixel, as well as their intensity value in each strip. The data were stored as CSV files and imported to R studio [56] for further processing. X coordinates of the pixels were converted into percentages relative to full length of the strip and the split into four segments corresponding to turns of cellulose/azo-xylan composites around the mandrel. Mean intensity values of each segment with the standard error of the mean from at least four replicated strips per treatment were plotted. Processing, analysis and plotting of the

data were done using Tidyverse 1.2.1, ggplot2 3.2.1, dplyr 0.8.3 R packages [56–59]. Code for extracting pixel information using Fiji and processing the data in R is deposited in GitHub and available through the link <https://github.com/mipavici/PACERassay>.

Assay for in-solution hydrolysis of azo-xylan

Xylanase reactions using azo-xylan were optimized to ensure absorbance values were within the linear range of the assay. Final reactions contained 0.06% azo-xylan in 50 mM sodium acetate buffer (pH 5.0). For activity assays using *NpXyn11A*, 0.001 mg/ mL *NpXyn11A* were used and incubations were performed at 40 °C and 300 rpm for 10 min. *NpXyn11A* activity on azo-xylan were also measured after pre-incubation of the azo-xylan solution with 0.003 mg/ mL *PcaLOOL2*, *PcaLOOL12* or *BSA* in a ThermoMixer C set at 25 °C and 300 rpm for 24 h. For activity assays using *Pm25* and corresponding variants, 0.03 mg/ mL *Pm25*, 0.03 mg/ mL *Pm25 Y213A Y378A* (aka M5), 0.017 mg/ mL *Pm25ΔCBMs* (aka M6) or 0.03 mg/ mL *Pm25 E546A* (aka M1) were used and reactions were incubated in a ThermoMixer C set at 40 °C and 300 rpm for 3, 6 and 20 h.

In all cases, reactions were terminated using 1 mL 96% (v/v) ethanol with vigorous stirring. In the case of reaction blanks, ethanol was added prior to enzyme addition. Supernatants were recovered by centrifugation (15,000 rpm for 10 min) and absorbance was analyzed spectrophotometrically at 590 nm.

Supplementary Information

The online version contains supplementary material available at <https://doi.org/10.1186/s13068-022-02128-8>.

Additional file 1: Figure S1. Impact of loosenin-like proteins on *NpXyn11A* hydrolysis of azo-xylan in solution. **Figure S2.** Impact of loosenin-like proteins on cellulose/azo-xylan composites. **Figure S3.** In-solution hydrolysis of azo-xylan by *Pm25* and its mutants. **Figure S4.** SDS-PAGE analysis of *CmXyn10B* (lane 2), *NpXyn11A* (lane 3) and *TfXyn11A* (lane 4). **Figure S5.** Replicate cellulose/azo-xylan composites after treatment for 1-h with (A) *NpXyn11A* or (B) *TfXyn11A*.

Acknowledgements

We thank Kuisma Littunen and Kim Kataja who assisted with substrate preparation and Nelly Monties who assisted with enzyme production. We also thank Professor A. McGuigan (University of Toronto) for helpful discussions.

Authors' contributions

MM prepared the cellulose/azo-xylan strips and conducted the experiments with the selected proteins with support from TK and VL. EJ established the method for preparing the cellulose/azo-xylan strips and validated the reproducibility of their construction. EJ also performed the preliminary experiments using the PACER assay. TP and MP performed the image analysis of strips used in the PACER assay. TE produced the *Pm25* enzymes used in the study and quantified their activity on soluble substrates. MM, EJ, TP, TK, VL, MP, TE, CD and ERM contributed to data interpretation. ERM conceived and coordinated the study and the writing process. All authors read and approved the final manuscript.

Funding

We thank the following granting agencies for their financial support: the European Research Council (ERC) (Consolidator Grant no. BHIVE – 648925) (MM, EJ, VL and ERM); Jenny and Antti Wihuri Foundation (Centre for Young Synbio Scientists) (TK); Academy of Finland Postdoctoral Researcher Grant No. 331853 (TP); The French national research agency (anr) Grant No. ANR-18-CES43-DECO (TE and CD).

Availability of data and materials

All data generated or analyzed during this study are reported in this manuscript and its Additional file 1.

Declarations

Ethics approval and consent to participate

Not applicable.

Consent for publication

Not applicable.

Competing interests

The authors have declared that no competing interests exist.

Author details

¹Department of Bioproducts and Biosystems, Aalto University, Kemistintie 1, 02150 Espoo, Finland. ²Department of Bioproduct Engineering, University of Groningen, Nijenborgh 4, 9747 AG Groningen, The Netherlands. ³Department of Agricultural Sciences, Viikki Plant Science Centre, University of Helsinki, P.O. Box 27, 00014 Helsinki, Finland. ⁴Toulouse Biotechnology Institute (TBI), Université de Toulouse, CNRS, INRAE, INSA, 31077 Toulouse, France. ⁵Department of Chemical Engineering and Applied Chemistry, University of Toronto, 200 College Street, Toronto, ON M5S 3E5, Canada.

Received: 18 November 2021 Accepted: 5 March 2022

Published online: 16 March 2022

References

- Bomble YJ, Lin CY, Amore A, Wei H, Holwerda EK, Ciesielski PN, Donohoe BS, Decker SR, Lynd LR, Himmel ME. Lignocellulose deconstruction in the biosphere. *Curr Opin Chem Biol.* 2017;41:61–70.
- Cragg SM, Beckham GT, Bruce NC, Bugg TD, Distel DL, Dupree P, Etxabe AG, Goodell BS, Jellison J, McGeehan JE, McQueen-Mason SJ, Schnorr K, Walton PH, Watts JE, Zimmer M. Lignocellulose degradation mechanisms across the Tree of Life. *Curr Opin Chem Biol.* 2015;2015(29):108–19.
- Hemsworth GR, Déjean G, Davies GJ, Brumer H. Learning from microbial strategies for polysaccharide degradation. *Biochem Soc Trans.* 2016;44:94–108.
- Jørgensen H, Kristensen JB, Felby C. Enzymatic conversion of lignocellulose into fermentable sugars: challenges and opportunities. *Biofuels Bioprod Biorefin.* 2007;1:119–34.
- Kumar B, Verma P. Enzyme mediated multi-product process: a concept of bio-based refinery. *Ind Crops Prod.* 2020;154:112607.
- Østby H, Hansen LD, Horn SJ, Eijsink VGH, Várnai A. Enzymatic processing of lignocellulosic biomass: principles, recent advances and perspectives. *J Ind Microbiol Biotechnol.* 2020;47:623–57.
- Guo H, Chang Y, Lee D-J. Enzymatic saccharification of lignocellulosic biorefinery: research focuses. *Biores Technol.* 2018;252:198–215.
- Singhvi MS, Chaudhari S, Gokhale DV. Lignocellulose processing: a current challenge. *RSC Adv.* 2014;4:8271–7.
- Viikari L, Vehmaanperä J, Koivula A. Lignocellulosic ethanol: from science to industry. *Biomass Bioenergy.* 2012;46:13–24.
- Arantes V, Saddler JN. Cellulose accessibility limits the effectiveness of minimum cellulase loading on the efficient hydrolysis of pretreated lignocellulosic substrates. *Biotechnol Biofuels.* 2011;4:3.
- Himmel ME, Ding SY, Johnson DK, Adney WS, Nimlos MR, Brady JW, Foust TD. Biomass recalcitrance: engineering plants and enzymes for biofuels production. *Science.* 2007;315:804–7.

12. Jeoh T, Ishizawa CI, Davis MF, Himmel ME, Adney WS, Johnson DK. Cellulase digestibility of pretreated biomass is limited by cellulose accessibility. *Biotechnol Bioeng*. 2007;98:112–22.
13. Karimi K, Taherzadeh MJ. A critical review on analysis in pretreatment of lignocelluloses: degree of polymerization, adsorption/desorption, and accessibility. *Bioresour Technol*. 2016;203:348–56.
14. Meng X, Ragauskas AJ. Recent advances in understanding the role of cellulose accessibility in enzymatic hydrolysis of lignocellulosic substrates. *Curr Opin Biotechnol*. 2014;27:150–8.
15. Arantes V, Saddler JN. Access to cellulose limits the efficiency of enzymatic hydrolysis: the role of amorphogenesis. *Biotechnol Biofuels*. 2010;3:4.
16. Leu S-Y, Zhu JY. Substrate-related factors affecting enzymatic saccharification of lignocelluloses: our recent understanding. *BioEnergy Res*. 2013;6:405–15.
17. Mansfield SD, Mooney C, Saddler JN. Substrate and enzyme characteristics that limit cellulose hydrolysis. *Biotechnol Prog*. 1999;15:804–16.
18. Siqueira G, Arantes V, Saddler JN, Ferraz A, Milagres AMF. Limitation of cellulose accessibility and unproductive binding of cellulases by pretreated sugarcane bagasse lignin. *Biotechnol Biofuels*. 2017;10:176.
19. Agrawal R, Verma A, Singhania RR, Varjani S, Dong CD, Patel AK. Current understanding of the inhibition factors and their mechanism of action for the lignocellulosic biomass hydrolysis. *Bioresour Technol*. 2021;332:125042.
20. Karuna N, Zhang L, Walton JH, Couturier M, Oztop MH, Master ER, McCarthy MJ, Jeoh T. The impact of alkali pretreatment and post-pretreatment conditioning on the surface properties of rice straw affecting cellulose accessibility to cellulases. *Bioresour Technol*. 2014;167:232–40.
21. Selig MJ, Thygesen LG, Felby C. Correlating the ability of lignocellulosic polymers to constrain water with the potential to inhibit cellulose saccharification. *Biotechnol Biofuels*. 2014;7:159.
22. Zhang J, Viikari L. Impact of xylan on synergistic effects of xylanases and cellulases in enzymatic hydrolysis of lignocelluloses. *Appl Biochem Biotechnol*. 2014;174:1393–402.
23. Grethlein HE. The effect of pore size distribution on the rate of enzymatic hydrolysis of cellululosic substrates. *Bio/Technology*. 1985;3:155–60.
24. Stone JE, Scallan AM, Donefer E, Ahlgren E. Digestibility as a simple function of a molecule of similar size to a cellulase enzyme. In: Hajny GJ, Reese ET, editors. *Cellulases and Their Applications*; 1969. Chap 13:219–241.
25. Chandra R, Ewanick S, Hsieh C, Saddler JN. The characterization of pretreated lignocellulosic substrates prior to enzymatic hydrolysis, part 1: a modified Simons' staining technique. *Biotechnol Prog*. 2008;24:1178–85.
26. Chandra RP, Ewanick SM, Chung PA, Au-Yeung K, Del Rio L, Mabee W, Saddler JN. Comparison of methods to assess the enzyme accessibility and hydrolysis of pretreated lignocellulosic substrates. *Biotechnol Lett*. 2009;31:1217–22.
27. Maloney TC. Thermoporosimetry of hard (silica) and soft (cellulosic) materials by isothermal step melting. *J Therm Anal Calorim*. 2015;121:7–17.
28. Donohoe DS, Resch MG. Mechanisms employed by cellulase systems to gain access through the complex architecture of lignocellulosic substrates. *Curr Opin Chem Biol*. 2015;29:100–7.
29. Eibinger M, Ganner T, Bubner P, Rošker S, Kracher D, Haltrich D, Ludwig R, Plank H, Nidetzky B. Cellulose surface degradation by a lytic polysaccharide monooxygenase and its effect on cellulase hydrolytic efficiency. *J Biol Chem*. 2014;289:35929–38.
30. Jeremic D, Goacher RE, Yan R, Karunakaran C, Master ER. Direct and up-close views of plant cell walls show a leading role for lignin-modifying enzymes on ensuing xylanases. *Biotechnol Biofuels*. 2014;7:496.
31. Novy V, Aïssa K, Nielsen F, Straus SK, Ciesielski P, Hunt CG, Saddler JN. Quantifying cellulose accessibility during enzyme-mediated deconstruction using 2 fluorescence-tagged carbohydrate-binding modules. *Proc Natl Acad Sci U S A*. 2019;116:22545–51.
32. Coughlan MP. The properties of fungal and bacterial cellulases with comment on their production and application. *Biotechnol Genet Eng Rev*. 1985;3:39–110.
33. Gourlay K, Arantes V, Saddler JN. Use of substructure-specific carbohydrate binding modules to track changes in cellulose accessibility and surface morphology during the amorphogenesis step of enzymatic hydrolysis. *Biotechnol Biofuels*. 2012;5:51.
34. Saloheimo M, Paloheimo M, Hakola S, Pere J, Swanson B, Nyssönen E, Bhatia A, Ward M, Penttilä M. Swollenin, a *Trichoderma reesei* protein with sequence similarity to the plant expansins, exhibits disruption activity on cellulosic materials. *Eur J Biochem*. 2002;269:4202–11.
35. Gourlay K, Hu J, Arantes V, Andberg M, Saloheimo M, Penttilä M, Saddler J. Swollenin aids in the amorphogenesis step during the enzymatic hydrolysis of pretreated biomass. *Bioresour Technol*. 2013;142:498–503.
36. Kang K, Wang S, Lai G, Liu G, Xing M. Characterization of a novel swollenin from *Penicillium oxalicum* in facilitating enzymatic saccharification of cellulose. *BMC Biotechnol*. 2013;13:42.
37. Quiroz-Castañeda RE, Martínez-Anaya C, Cuervo-Soto LI, Segovia L, Folch-Mallol JL. Loosenin, a novel protein with cellulose-disrupting activity from *Bjerkandera adusta*. *Microb Cell Fact*. 2011;10:8.
38. Liu X, Ma Y, Zhang M. Research advances in expansins and expansion-like proteins involved in lignocellulose degradation. *Biotechnol Lett*. 2015;37:1541–51.
39. Kim ES, Lee HJ, Bang W-G, Choi I-G, Kim KH. Functional characterization of a bacterial expansin from *Bacillus subtilis* for enhanced enzymatic hydrolysis of cellulose. *Biotechnol Bioeng*. 2009;102:1342–53.
40. Qin YM, Tao H, Liu YY, Wang YD, Zhang JR, Tang AX. A novel non-hydrolytic protein from *Pseudomonas oryzaehabitans* enhances the enzymatic hydrolysis of cellulose. *J Biotechnol*. 2013;168:24–31.
41. Quarantin A, Castiglioni C, Schäfer W, Favaron F, Sella L. The *Fusarium graminearum* cerato-platanins loosen cellulose substrates enhancing fungal cellulase activity as expansin-like proteins. *Plant Physiol Biochem*. 2019;130:229–38.
42. Hu J, Tian D, Rennecker S, Saddler JN. Enzyme mediated nanofibrillation of cellulose by the synergistic actions of an endoglucanase, lytic polysaccharide monooxygenase (LPMO) and xylanase. *Sci Rep*. 2018;8:3195.
43. Rodenhizer D, Gaude E, Cojocari D, Mahadevan R, Frezza C, Wouters BG, McGuigan AP. A three-dimensional engineered tumour for spatial snapshot analysis of cell metabolism and phenotype in hypoxic gradients. *Nat Mater*. 2016;15:227–34.
44. Wu H, Ioannou E, Henrissat B, Montanier CY, Bozonnet S, O'Donohue MJ, Dumon C. Multimodularity of a GH10 xylanase found in the termite gut metagenome. *Appl Environ Microbiol*. 2021;87:e01714-e1720.
45. Scheller HV, Ulvskov P. Hemicelluloses. *Annu Rev Plant Biol*. 2010;61:263–89.
46. Irwin D, Jung ED, Wilson DB. Characterization and sequence of a *Thermomonospora fusca* xylanase. *Appl Environ Microbiol*. 1994;60:763–79.
47. Biely P, Vršanská M, Tenkanen M, Kluepfel D. Endo- β -1,4-xylanase families: differences in catalytic properties. *J Biotechnol*. 1997;57:151–66.
48. Karlsson EN, Schmitz E, Linares-Pastén JA, Adlercreutz P. Endo-xylanases as tools for production of substituted xylooligosaccharides with prebiotic properties. *Appl Microbiol Biotechnol*. 2018;102:9081–8.
49. Boraston AB, Bolam DN, Gilbert HJ, Davies GJ. Carbohydrate-binding modules: fine-tuning polysaccharide recognition. *Biochem J*. 2004;382:769–81.
50. Gilbert HJ, Knox JP, Boraston AB. Advances in understanding the molecular basis of plant cell wall polysaccharide recognition by carbohydrate-binding modules. *Curr Opin Struct Biol*. 2013;23:669–77.
51. Suzuki H, Vuong TV, Gong Y, Chan K, Ho CY, Master ER, Kondo A. Sequence diversity and gene expression analyses of expansin-related proteins in the white-rot basidiomycete, *Phanerochaete carnosus*. *Fungal Genet Biol*. 2014;72:115–23.
52. Cosgrove DJ. Microbial expansins. *Annu Rev Microbiol*. 2017;71:479–97.
53. Bastien G, Arnal G, Bozonnet S, Laguerre S, Ferreira F, Fauré R, Henrissat B, Lefèvre F, Robe P, Bouchez O, Noirot C, Dumon C, O'Donohue M. Mining for hemicellulases in the fungus-growing termite *Pseudacanthotermes militaris* using functional metagenomics. *Biotechnol Biofuels*. 2013;6:78.
54. Rueden CT, Schindelin J, Hiner MC, DeZonia BE, Walter AE, Arena ET, Eliceiri KW. ImageJ2: imageJ for the next generation of scientific image data. *BMC Bioinformatics*. 2017;18:529.
55. Schindelin J, Arganda-Carreras I, Frise E, Kaynig V, Longair M, Pietzsch T, Preibisch S, Rueden C, Saalfeld S, Schmid B, Tinevez JY, White DJ, Hartenstein V, Eliceiri K, Tomancak P, Cardona A. Fiji: an open-source platform for biological-image analysis. *Nat Methods*. 2012;9:676–82.
56. R Core Team. R: a language and environment for statistical computing. R Found Stat Comput; 2019.
57. Wickham H. ggplot2: Elegant Graphics for Data Analysis. J R Stat Society: Series A (Statistics in Society); 2016.
58. Wickham H. Package "tidyverse" for R: Easily Install and Load the "Tidyverse." R Packag. version 1.2.1. 2017.

59. Wickham H, François R, Henry L, Müller K. dplyr: A Grammar of Data Manipulation. R package version. Media; 2019.

Publisher's Note

Springer Nature remains neutral with regard to jurisdictional claims in published maps and institutional affiliations.

Ready to submit your research? Choose BMC and benefit from:

- fast, convenient online submission
- thorough peer review by experienced researchers in your field
- rapid publication on acceptance
- support for research data, including large and complex data types
- gold Open Access which fosters wider collaboration and increased citations
- maximum visibility for your research: over 100M website views per year

At BMC, research is always in progress.

Learn more biomedcentral.com/submissions

